

# Land-use perturbations in ley grassland decouple the degradation of ancient soil organic matter from the storage of newly derived carbon inputs.

5 Marco Panettieri<sup>1,2</sup>, Denis Courtier-Murias<sup>3</sup>, Cornelia Rumpel<sup>4</sup>, Marie-France Dignac<sup>4</sup>, Gonzalo Almendros<sup>2</sup>, and Abad Chabbi<sup>1,5</sup>

<sup>1</sup>INRAE, AgroParisTech, UMR1402 ECOSYS, F-78850 Thiverval-Grignon, France

<sup>2</sup>Museo Nacional de Ciencias Naturales (MNCN-CSIC), c/Serrano 115-B, 28006, Madrid, Spain

<sup>3</sup>GERS-LEE, Univ Gustave Eiffel, IFSTTAR, F-44344 Bouguenais, France

<sup>4</sup>CNRS, IEES UMR (UPMC, CNRS, UPEC, IRD, INRAE)

10 <sup>5</sup>INRAE, UR P3F, 86600 Lusignan, France

*Correspondence to:* Abad Chabbi (abad.chabbi@inrae.fr)

**Abstract.** In a context of global change, soil has been identified as a potential carbon (C) sink, depending on land-use strategies. To detect the trends of carbon stocks after the implementation of new agricultural practices, early indicators, which can highlight changes in short timescales are required.

15 This study proposes the combined use of stable isotope probing and chemometrics applied to solid-state <sup>13</sup>C NMR spectra to unveil the dynamics of storage and mineralization of soil C pools. We focused on light organic matter fractions isolated by density fractionation of soil water stable aggregates because they respond faster to changes in land-use than the total soil organic matter. Samples were collected from an agricultural field experiment with grassland, continuous maize cropping, and ley grassland under temperate climate conditions.

20 Our results indicated contrasting aggregate dynamics depending on land-use systems. Under our experimental conditions, grassland returns larger amount of C as belowground inputs than maize cropping, evidencing a different distribution of light C fractions between aggregate classes. Coarse aboveground inputs from maize were contributing mostly to larger macroaggregates, Land-use changes with the introduction of ley grassland provoked a decoupling of the storage/degradation processes after the grassland phase. The newly-derived maize inputs were barely degraded during the first three years of maize  
25 cropping, whereas grassland-derived material was depleted. As a whole, results suggest large microbial proliferation as showed by <sup>13</sup>C NMR under permanent grassland, then reduced within the first years after the land-use conversion, and finally restored. The study highlighted a fractal structure of the soil determining a scattered spatial distribution of the cycles of storage and degradation of soil organic matter related to detritosphere dynamics. In consequence, vegetal inputs from a new land-use are creating new detritosphere microenvironments that may be disconnected from the dynamics of C cycle of the previous land-  
30 use. The formation of those different and unconnected microenvironments may explain the observed legacy effect of the

previous land-use, since each microenvironment type contributes separately to the overall soil C cycle. The effect of the new land-use on soil C cycle are delayed until the different detritosphere microenvironments remain unconnected and the ones from the previous land-use represent the predominant microenvironment type. Increasing the knowledge on the soil C dynamics at fine scale will be helpful to refine the prediction models and land-use policies.

## 35 **1 Introduction**

Soil carbon (C) stocks represent the largest C pool of the terrestrial biosphere (Scharlemann et al., 2014), which is accumulated or released to the atmosphere to an extent dependent on land-use and anthropogenic factors (Lal, 2004; Powlson et al., 2011). In fact, soil has the potential to store a large amount of C but also to emit great quantity of greenhouse gases (GHG) depending on management practices (Lal, 2008; Smith, 2016). Agriculture is responsible for 20% of total GHG emission, but the  
40 transformation of soil into a C sink with sustainable agricultural practices (Chenu et al., 2019) has been proposed as a promising mitigation strategy by researchers, international panels and governments (IPCC, 2013; Lal, 2008; Minasny et al., 2017). These mitigation strategies need to be evaluated using adequate biomarkers that can decipher the stabilization/destabilization mechanisms and in particular the direction of change of the suitable land-use practices (Dignac et al., 2017; Wiesmeier et al., 2019), and refine the prediction models about C balance associated with land-use policies (Chenu et al., 2019).

45 Changes in land-uses affect soil C stocks on a timescale of years or decades, therefore early modifications in SOM dynamics may be undetectable when the quantification of soil C contents is performed on total soil rather than on reactive SOM pools (Castellano et al., 2015; Panettieri et al., 2017; Wiesmeier et al., 2019).

In a context of land-use change, chemical characterization and stable isotope probing of SOM will establish biochemical decomposition patterns and C turnover rates, but the complex nature of SOM requires high-end analytical techniques (Derenne  
50 and Nguyen Tu, 2014), such as solid-state  $^{13}\text{C}$  nuclear magnetic resonance (NMR) or stable isotope probing (SIP). For soils that have experienced a land-use change with a conversion from C3 to C4 vegetation, the use of SIP is a valid method to measure the turnover of bulk SOM (Balesdent et al., 1987; Dignac et al., 2005) and specific SOM pools (Bol et al., 2009; Matos et al., 2011; Yamashita et al., 2006). The turnover rate of SOM pools is also affected by the type and the quality of litter returned to soil, which is land-use specific (Armas-Herrera et al., 2016; von Haden et al., 2019). However, the litter chemical  
55 composition and its mineralization pattern are the two main proxies of SOM quality that can be assessed with solid-state  $^{13}\text{C}$  NMR (Baldock and Preston, 1995; Knicker et al., 2012). Solid-state  $^{13}\text{C}$  NMR analysis of chemically or physically isolated SOM pools has been used to evaluate the degradation status of SOM induced by land-use (Rabbi et al., 2014) and agricultural management (Panettieri et al., 2013, 2014).

However, establishing an adequate field experiment to assess the effect of management practices on long-term C storage in  
60 the soil is not a trivial task. Most of the research on soils conducted at the aggregate or molecular scales has been based on

laboratory incubation conditions or with a limited experimental time (Dignac et al., 2017). Therefore, the extrapolation of those results to larger scales, longer intervals of time and more diverse soil conditions (land-uses, physical and chemical characteristics) is always arbitrary.

In this study we focused on the implementation of ley grassland rotations, which have been identified as a way to store carbon and provide ecosystem services (Kunrath et al., 2015; Lemaire et al., 2014). Few field studies have been targeted on the long-term effects of ley grassland on soil organic matter (SOM) dynamics (Crème et al., 2018; Panettieri et al., 2017; Solomon et al., 2007). The combination of two different land-uses (grassland and maize cropping) in a nine-year ley grassland rotation produces differences in C contents at the arable layer are only detectable at the aggregate scale, whereas bulk soil did not show significant change (Panettieri et al., 2017). Thus, to detect the magnitude and the direction of the land-use dependant changes of SOM dynamics, SOM pools with a short turnover time are needed.

In consequence, the present research has been focused on the characterization of the light fraction of SOM (LF, particulate organic matter), i.e. a fraction that has been identified as an early indicator for changes in land-use having a faster turnover time than mineral associated organic matter (Courtier-Murias et al., 2013; Leifeld and Kögel-Knabner, 2005; Panettieri et al., 2014). The present study has been designed to identify the processes affecting the labile soil C pools resulting from changes in land-use. A temporary (ley) grassland system was compared with permanent grassland, permanent cropland and bare fallow soils as controls using a novel approach based on combination of stable isotopes analysis and  $^{13}\text{C}$  NMR spectroscopy. To date, the combined use of SIP and  $^{13}\text{C}$  NMR on soil LF to assess the effect of changes of land-use on agricultural soils is scarce (Helfrich et al., 2006).

The hypothesis of this work is that the composition of LF provides early information about the direction and magnitude of the change affecting SOM stocks in terms of accumulation or mineralization, which depend on the litter nature (above vs. belowground biomass) and land-use characteristics (cropping vs. grassland). To test this hypothesis, the chemical composition of LF isolated from different water stable aggregates (Plaza et al., 2012) was characterized by solid-state  $^{13}\text{C}$  NMR spectroscopy. The obtained information was combined with measures of LF turnover in soil assessed by the natural abundance  $^{13}\text{C}$  enrichment of SOM provided by the in situ labelling of maize crops in a nine-year field experiment in western France.

## 2 Materials and methods

### 2.1 Experimental area

Soil samples were collected from the long-term experiment “Systems of Observation and Experimentation in Environmental Research-Agro-ecosystem, Biogeochemical Cycles and Biodiversity (SOERE-ACBB)” hosted at INRAE-Lusignan facilities (46°25'12.91" N; 0°07'29.35" E) in western France (Fig. 1).

90 The pedoclimatic characteristics of the studied area have been extensively described elsewhere (Chabbi et al., 2009; Moni et al., 2010). In summary, the area has a temperate climate with around 846 mm of annual precipitation, average annual temperature of 11.9 °C. The soil texture of upper soil horizons is a loamy, Cambisol (130 g kg<sup>-1</sup> sand, 692 g kg<sup>-1</sup> silt, 177 g kg<sup>-1</sup> clay), while lower soil horizons are clayed rubefied with high content of kaolinite and oxides, classified as a Paleo-Ferralsol (103 g kg<sup>-1</sup> sand, 612 g kg<sup>-1</sup> silt, 286 g kg<sup>-1</sup> clay). The soil bulk density was 1.48 g cm<sup>-3</sup> (0–30 cm) with a pH(H<sub>2</sub>O) of 6.3 and  
95 11 g kg<sup>-1</sup> of organic carbon in the first 30 cm.

The long-term experiment started in 2005, on an area previously covered by oak forest and then devoted to agriculture or grassland for at least 100 years.

A total of four treatments representing different land-uses were distributed on a 10 ha area with four replicates per treatment arranged in four randomized blocks (one replicate per treatment in each block of about 4000 m<sup>2</sup>). Four different treatments  
100 were selected for sampling in the framework of the present experiment: (i) permanent crop rotations (PC), (ii) permanent grassland (PG), (iii) ley grassland (LG, 6 years of grassland followed by 3 years of continuous cropping), and (iv) bare fallow (BF). To take advantage of the *in situ* <sup>13</sup>C labelling of SOM induced by maize plant inputs, only the subplots (500–700 m<sup>2</sup>) cultivated under maize (*Zea mays* L.) of PC and LG, were sampled (9 years under continuous maize for PC, and 6 years under grassland followed by 3 years under maize, for LG). Grassland plots were sown with three dominant species *Lolium perenne*  
105 L. (cv Milca), *Festuca arundinacea* Scriber (cv Soni), and *Dactylis glomerata* L. (cv Ludac) and hay was harvested and exported three times per year. Before each maize growing cycle, soil was tilled with a mouldboard plough at 25–30 cm depth yearly, followed by minor tillage operations before maize sowing (1 crop per year). All the treatments, except bare fallow subplots, were N fertilized. Grassland received between 170 and 380 kg N ha<sup>-1</sup> year<sup>-1</sup> (on average 240 kg ha<sup>-1</sup> y<sup>-1</sup>), targeting the nitrogen nutrition index (NNI) between 0.9 and 1 (Lemaire et al., 2008). Maize crops were fertilized following local  
110 agronomic practices and received between 36 and 160 kg N ha<sup>-1</sup> year<sup>-1</sup> (on average 98 kg N ha<sup>-1</sup> y<sup>-1</sup>). Finally, subplots of bare fallow were 54 m<sup>2</sup> wide without any input from vegetation or fertilization.

## 2.2 Sampling and aggregate fractionation

In July 2014, 20 cm diameter stainless steel cylinders were used to collect soil samples limiting aggregate disruption at a 0–  
115 30 cm depth, corresponding to the layer affected by tillage operations. Five soil cores were sampled for each plot at least 1 m far from the edges (three cores in the case of bare fallow subplots) and immediately merged to obtain a composite sample. Further information about the sampling procedure was reported in previous work (Panettieri et al., 2017).

Water content of bulk soil subsamples was determined gravimetrically right after the sampling, and then soil was dried at room temperature before fractionation.

120 Water stable aggregates were isolated from bulk soil samples rewetted by slaking following the method of modified by Le  
Bissonnais (1996). Briefly, larger clods and plant debris ( $\varnothing > 7.1$  mm) were discarded and soil was left to slake for capillarity  
on a sand/kaolinite basin for 1 h. Successively, 50 g of soil were placed on a 2 mm mesh sieve, submerged in deionised water  
and sieved for 2 min. The sieve was oscillated 50 times with a vertical excursion of  $\sim 3$  cm. The soil suspension was passed  
through the other sieves to obtain four soil aggregate fractions: larger macroaggregates (LMA,  $\varnothing 2\text{--}7.1$  mm), macroaggregates  
125 (MA,  $\varnothing 0.2\text{--}2$  mm), microaggregates (miA,  $\varnothing 0.05\text{--}0.2$ ) and silt and clay-size aggregates (S+C,  $\varnothing < 0.050$  mm). On average,  
the mass recovery was 98%, and not lower than 93% for all the samples. The mean weight diameter (MWD) for the four  
treatments were calculated following the method of van Bavel (1950):

$$MWD = \sum_{i=1}^n \bar{D}_i \times f_i \quad (1)$$

In which  $n$  is the number of aggregate classes,  $f_i$  is the relative abundance of the aggregate class, and  $\bar{D}_i$  is the arithmetic mean  
130 between the upper and lower limit of the aggregate class.

### 2.3 Isolation of light fractions of SOM

The light fraction (LF) was isolated as the floating fraction during wet sieving for each aggregate sample, including the free  
and occluded sub-fractions. LF was extracted from soil samples using the method described by Kölbl and Kögel-Knabner  
(2004), modified to fit the experimental condition of this study. Briefly, 20 g of bulk soil samples or aggregate fractions were  
135 placed in a plastic vessel cooled by a water stream on external walls to dissipate the heat. Samples were dispersed in 200 mL  
of a sodium polytungstate (SPT,  $3\text{Na}_2\text{WO}_4 \cdot 9\text{WO}_3 \cdot \text{H}_2\text{O}$ , MW: 2986.01 g mol<sup>-1</sup>, Sigma-Aldrich) solution at a density of 1.8  
g cm<sup>-3</sup> using an ultrasonic probe (Scientific Bioblock Vibra-Cell 75115) calibrated to apply a power of 450 J mL<sup>-1</sup>, as described  
by Poeplau and Don (2014). After sonication, vessels were allowed to settle down overnight and total LF (free and occluded)  
was separated from the mineral phase by centrifugation at 1000 g. The LF samples were recovered using a pressure filtration  
140 system on a cellulose-free membrane filter (0.45  $\mu\text{m}$  pore size Pall Life Science Supor® 450) and successively washed with  
deionized water to remove all the SPT residues, until conductivity became lower than 5  $\mu\text{S cm}^{-1}$ . Finally, samples were freeze  
dried and adequately stored.

For the present work, bulk soil samples from three blocks were analysed individually for each treatment (for a total of 12 bulk  
soil samples), whereas, for aggregate fractions, field replicates were merged in a composite sample (one aggregate fraction per  
145 treatment, for a total of 16 samples) to overcome constraints regarding quantity of fractions recovered and NMR instrumental  
time.

## 2.4 Organic C and isotopic $\delta^{13}\text{C}$ signature of samples

The experimental area was dominated by C3 vegetation and the soil  $\delta^{13}\text{C}$  signature at the beginning of the experiment was -25‰ relative to Vienna Pee Dee Belemnite (VPDB) standard.

- 150 The determination of total organic C (TOC), total N (TN) and  $^{13}\text{C}$  isotopic signatures of all the LF samples were performed on dry aliquots using an isotopic ratio mass spectrometer (VG SIRA 10) coupled to an elemental analyser (CHN NA 1500, Carlo Erba). The isotopic  $^{13}\text{C}/^{12}\text{C}$  ratios ( $\delta^{13}\text{C}$ ) were calibrated against the VPDB standard and expressed with equation (2):

$$\delta^{13}\text{C} = \left( \frac{(^{13}\text{C}/^{12}\text{C})_{\text{sample}}}{(^{13}\text{C}/^{12}\text{C})_{\text{VPDB}}} - 1 \right) \times 1000 \quad (2)$$

- 155 The turnover of LF carbon (LF-C) was quantified using the  $^{13}\text{C}$  enrichment induced by maize crops in plots under permanent cropland and ley grassland as described by Balesdent and Mariotti (1996), simplified as described by Dignac et al. (2005), equation (3):

$$F = \frac{\text{LFC}_{\text{new}}}{\text{LFC}} = \frac{\delta_{\text{soilM}} - \delta_{\text{soilG}}}{\delta_{\text{newM}} - \delta_{\text{newG}}} \quad (3)$$

in which LFC refers to total C quantity within the soil LFC, and  $\text{LFC}_{\text{new}}$  refers to C quantity within the LF-C derived from the new maize vegetation.

- 160 For the isotopic ratios ( $\delta$ ), the subscript *soilM* stands for the soil  $\delta^{13}\text{C}$  measured for the two plots under maize (9 years of maize for permanent cropland, and 3 years of maize after ley grassland), *soilG* stands for permanent grassland controls under continuous C3 vegetation, *newM* and *newG* stand for the isotopic composition of maize and grass vegetal material. To estimate the term ( $\delta_{\text{newM}} - \delta_{\text{newG}}$ ), the difference in isotopic composition between plant materials corrected for above and below ground inputs to soil was used, as calculated in a previous study on the same experimental farm (Panettieri et al., 2017). Using the
- 165 values of *F*, the percentage of C3-derived organic matter remaining in samples from ley grassland and permanent cropland was calculated with reference to the permanent grassland samples. Similarly, degradation of LF in absence of new vegetal inputs was calculated from bare fallow samples. This approach produced an index of C3-LF persistence under different land-uses.

## 2.5 Solid-state $^{13}\text{C}$ Nuclear Magnetic Resonance

- 170 The  $^{13}\text{C}$  NMR analyses were carried out on a Bruker Avance 400 spectrometer operating at a  $^{13}\text{C}$  frequency of 100.6 MHz employing a  $^{13}\text{C}$  ramped amplitude Cross Polarization Single Pulse sequence under Magic Angle Spinning conditions (Ramp-CPSP/MAS). This sequence was first introduced by Shu et al. (2010) in material sciences, then successfully applied by Courtier-Murias et al. (2014) on environmental samples. Spectra of LF samples obtained with a standard cross polarization

(Ramp-CP/MAS) sequence with an equal number of scans (i.e. the same acquisition time) were compared at the beginning of the experiment (Supplementary Fig. S1). Preliminary experiment showed that Ramp-CPSP/MAS outperformed Ramp-CP/MAS (CP, hereafter) in terms of signal-to-noise ratio by a factor of ca. ~2, in spectral regions with a lower proton density, i.e. the aromatic region. Therefore, only Ramp-CPSP/MAS (CPSP, hereafter) analyses were carried out for the whole sample set.

Approximately 50–100 mg of sample were placed into a zirconium oxide rotor with a diameter of 4 mm and sealed with Kel-F® caps. For all the measurements, a spinning speed of 10 kHz was applied, the contact time was set to 1 ms and the recycle delay was 3 s; this value was higher than in our previous works (Courtier-Murias et al., 2014) due to the technical specifications of the NMR probe used in this study. About 5000–10000 scans were accumulated for each sample and a ramped  $^1\text{H}$  pulse was used during Hartmann-Hahn contact to circumvent Hartmann-Hahn mismatches. The spectra were divided in 8 main regions, assignments for carbon resonances are reported in Table 1 according to Knicker and Lüdemann (1995) and Knicker (2011).

## 2.6 Statistical analyses

A Shapiro-Wilk test was used to check data normality before further analyses. For bulk soil and LF isolated from bulk soil samples, the significance of the differences found for the variables ( $P \leq 0.05$ ) induced by the four land-uses was assessed by non-parametric Kruskal-Wallis tests and the Dunn's multiple pairwise comparisons. For the NMR analyses, significance was assessed on bulk soil samples, whereas on composite samples, significance was not assessed due to the lack of replicate measurements. The significance level of Spearman's correlation coefficient ( $\rho_s$ ) between the measured variables were assessed at a significance level of  $P \leq 0.05$ . A Principal Component Analysis (PCA) was used to explore how the chemical composition assessed by NMR affected sample distribution by groups. Since integrals of NMR regions are compositional data (their sum is the total measured intensity), data were pre-treated to reduce the effect of collinearity using the principles of Aitchinson's geometry and center logratio transformed (CLR) prior to the PCA calculation (Aitchison, 1982). Total organic carbon (TOC), carbon to nitrogen ratios (C/N) and C3-derived LF-C losses were used as supplementary variables. Statistical analyses were carried out using XLSTAT (Addinsoft, Boston, USA, <https://www.xlstat.com>).

A chemometrics approach was used to treat NMR spectra and obtain information about the relative contribution of C3 and C4-derived organic matter to LF fractions. Spectra were exported as a 2-column matrix reporting chemical shift (516 points corresponding to about 2 points per ppm) and absolute intensity for each point. Afterwards, normalized intensities ( $I_f$ ) were calculated to overcome the different C contents of each sample that may lead to different signal to noise ratios for each spectrum following equation (4) and (5).

$$I_t = \sum_{n=1}^{516} I_n \quad (4)$$

$$I_f = I_n \div I_t \times 1000 \quad (5)$$

Measured intensities at each point ( $I_n$ ) were divided by the total spectrum intensity ( $I_t$ ) calculated as the sum of the intensities for each point ( $n= 516$ ) then multiplied by an arbitrary factor of 10000 to keep the normalized intensities within a range of -2 to 40.

Normalized intensities were used to obtain scaled spectra, one for each sample. Afterwards, the samples of permanent grassland were chosen as reference spectra (free of C4-derived SOM and with continuous vegetal inputs) whereas spectra from other treatments were subtracted from the corresponding permanent grassland sample spectra. This leads to a graphical view on changes in LF originated by different land-uses, with positive signal for the regions in which permanent grassland had higher relative contribution than the subtracted treatment, and negative signal for the opposite situation.

### 3 Results and discussion

#### 3.1 Carbon contents in total soil and light fractions

The LF-C contents represented between 7 and 30% of the TOC for bulk soil and aggregates (Fig. 2), in line with results of other studies (Leifeld and Kögel-Knabner, 2005). No significant differences in the relative contributions of LF-C to TOC between the four treatments were highlighted for bulk soil samples (Fig. 2). Larger macroaggregates showed the highest LF-C contribution among the fractions (Fig. 2), and trends toward higher relative contribution of LF-C to TOC were found for permanent cropland samples compared with the corresponding fractions of the other treatments. Ley grassland induced a decrease of the LF-C contents of the bulk soil, the larger macroaggregates and the microaggregates fractions if compared with permanent grassland and permanent cropland homologous fractions (Fig. 2). Bearing in mind the relative contribution of LF-C to TOC, LF-C has been proposed as an early indicator of changes affecting soil quality due to the faster turnover than TOC, normally on a timespan of years (Poeplau et al., 2018). This useful characteristic has been proposed to detect changes in C stocks modulated by land-use against the large background of TOC that is not affected (Leifeld and Kögel-Knabner, 2005). The LF-C contents under ley grassland decreased to level comparable to those measured for bare fallow in which no vegetal inputs were returned to soil during the previous nine years. We attribute these results to the effect of soil perturbation due to the switch from a grassland soil ecosystem to a crop soil ecosystem. Maize cropping includes deep tillage operations and provides a different type of vegetal inputs: grassland is characterized by an extended, dense and relatively shallow root system, whereas maize roots are more spaced and deep (Jackson et al., 1996).

On the one hand, cropping produces changes in soil aggregation (Álvaro-Fuentes et al., 2008; Bronick and Lal, 2005) which are associated with LF-C degradation due to the increase of microbial activity (Courtier-Murias et al., 2013; Panettieri et al., 2014) and changes in physical protection that soil aggregates provide to land-use specific proportion of LF-C (Leifeld and Kögel-Knabner, 2005).



On the other hand, previous studies on the same experimental area reported that grassland total inputs to soil were higher than those from maize crops, but the type and distribution of those inputs presented meaningful differences (Panettieri et al., 2017; 235 Armas-Herrera et al., 2016). Maize returned a larger proportion of aboveground biomass, successively incorporated into soil during tillage, and a lower percentage of root-derived material, whereas grassland provides a large proportion of belowground inputs to soil in a more extended area.

Despite the higher number of tillage operations performed under ley grassland and permanent cropland, the MWD was significantly higher for permanent cropland compared with bare fallow (Table 2). No significant differences were found 240 between permanent cropland and the two grassland systems due to large data dispersion, even if a trend towards lower MWD for ley grassland and permanent grassland was highlighted (Table 2). Given that grassland returns to soil a larger amount of belowground inputs than maize crops, we can suggest that such incorporation takes place at the level of smaller size aggregates richer in C, in comparison with the incorporation into coarser aggregates of C originating from maize crops.

### 3.2 Local proxies of soil organic matter dynamics

245 The use of stable isotope probing allowed to distinguish the percentages of C4-derived material proceeding from maize vegetal inputs from the C3-derived material in the LF-C extracted from soils under ley grassland and permanent cropland (Fig. 3). The latter showed higher proportions of C4-derived LF-C than ley grassland within all the aggregate fractions, due to the longer time cropped under maize. LF-C from silt and clay fraction was mostly composed of C3-derived C, less than 5% of new C was found for permanent cropland and no new inputs were detected for ley grassland. The contribution of new C in the LF 250 increased with aggregate size for all the fractions of permanent cropland; 31% of LF-C in larger macroaggregates of permanent cropland was maize-derived, evidencing the faster turnover of larger aggregates, which has been extensively described in the literature and correspond to the preferential accumulation of particulate, slightly decomposed LF in coarse soil fractions (Puget et al., 1995, 2000; Tisdall and Oades, 1982). The contribution of maize-derived material increased with aggregate size for permanent cropland, whereas a different trend was observed for ley grassland treatment. The contribution of new C to the LF 255 of larger macroaggregates was similar to that of permanent cropland, however, the contributions of maize-derived C to the LF-C of macroaggregates and microaggregates of ley grassland were very similar, representing a break in the linear pattern found for ley grassland (Fig. 3).

Taking into account the total amount of LF-C (C3 and C4-derived), Fig. 4 shows that the larger macroaggregates and microaggregates of ley grassland contained the lowest amount of LF-C if compared with all the treatments, a different trend 260 than that observed for permanent cropland. These results showed that a three-year continuous maize cropping following a six-year grassland produced severe disruption and/or rearrangement of C pools. The measured losses of LF-C under ley grassland were not supported by similar losses of TOC, therefore the tillage operations and maize cropping may have led to redistribution of this C, favouring its incorporation into heavier mineral associated C-pools (Basile-Doelsch et al., 2009). Such LF-C losses

are not attributable to maize cropping, since the observed trends for soils under permanent maize suggested that longer time  
265 of maize cropping will restore the depleted LF-C of larger macroaggregates and microaggregates. Moreover, losses of C3-  
derived LF-C were not registered for plots under permanent maize. Only two pools of LF-C have been partitioned using the  
 $^{13}\text{C}$  *in situ* labelling, but we cannot exclude that the C3-derived LF-C is on its turn composed of different land-use specific  
pools accumulated before the establishment of the experiment (DeGryze et al., 2004; Meyer et al., 2012). Those pools may  
have been more susceptible to alteration by the land-use changes from grassland to maize, but not to continuous maize  
270 cropping. Since no further isotopic partitioning is possible on the LF-C accumulated before the beginning of the experiment,  
chemical composition of LF-C pools assessed by solid-state  $^{13}\text{C}$  NMR will be used to provide further insights about the effect  
of land-use change on C stocks.

### 3.3 Performance of the NMR method

To test the performance of CPSP sequence against the more commonly used CP, two spectra from the same sample were  
275 acquired using the same number of scans for both experiments. Fig. S1 shows that CPSP sequences was able to detect a higher  
intensity of the signal for aromatic-C in comparison with CP sequence, with negligible modifications detected for the other  
regions. This is due to the lower proton density in condensed aromatic moieties, that can lead to a less effective polarization  
transfer from proton to carbon nuclei. In CP experiments, an increase of the contact time to transfer the magnetization along  
the distance between condensed aromatic-C and closest proton could be used as a solution to overcome this problem. However,  
280 longer contact times are also correlated with losses of signal intensity mediated by the spin-lattice relaxation, which will  
produce lower signal intensity (Knicker, 2011). The extra  $^{13}\text{C}$  pulse of the CPSP sequence allows to better measure  $^{13}\text{C}$  atoms  
of the condensed aromatic moieties that are far from protons and therefore improving the signal-to-noise ratio of this region  
especially when their  $^{13}\text{C}$  NMR  $T_1$  relaxation values are short (Courtier-Murias et al., 2014). In addition, some differences for  
 $\text{CH}_2$  groups in non-crystalline poly(methylene) and carbonyls groups have also been detected (Courtier-Murias et al., 2014).  
285 However, CPSP always equals or improves CP performance even for soils with a low aromaticity, as confirmed for our  
comparison spectra. In consequence, CPSP was therefore selected as the standard sequence for this study.

Standard deviations of the calculated areas for the field replicates (three different blocks) of bulk soil samples were lower than  
1.35% for all the integrated regions, except for *O*-alkyl C region of permanent grassland (2.05 %). This assessed that the  
variability due to spatial conditions and sample preparation was reasonably low and the integrated areas of the spectra from  
290 the composite samples are valid to be interpreted in terms of differences in SOM in the different aggregate fractions.

Contributions in carboxyl C and *N*-alkyl C were constant (7–9 % and 9–10 %, respectively) for all the measured samples, with  
the exception of bare fallow samples, in which carboxyl C accounted for more than 10% in larger macroaggregates and  
microaggregates. The region assigned to *N*-alkyl C may also represent the typical signal assigned to methoxyl C of lignin  
structures (Lüdemann and Nimz, 1973). Signal intensity in the *N*-alkyl region showed a significant positive Spearman's

295 correlation with total N content ( $\rho_s = 0.647$ ,  $P < 0.05$ ) and a significant negative correlation with the intensity of the heteroaromatic C region ( $\rho_s = -0.574$ ,  $P < 0.05$ ), suggesting that the *N*-alkyl signal is derived mainly from C in proteinaceous material rich in N rather than methoxyl C. The persistence of protein derived material in SOM pools has been described in other studies (Diekow et al., 2005; Nannipieri and Eldor, 2009; Panettieri et al., 2014) and it has been used to characterize LF as “new” SOM, rich in fresh litter, but also exoenzymes and cytoplasmic material from microbial biomass and necromass  
300 (Miltner et al., 2012).

The alkyl-to-*O*-alkyl C ratio is commonly used as a proxy of SOM degradation (Baldock and Preston, 1995). Isotopic results showed how larger aggregates contain fresher LF-C, confirmed by the decrease of the alkyl/*O*-alkyl with the increase of aggregate size. Fresh litter is richer in carbohydrates from cellulose which anomeric C resonates in the *O*-alkyl region, whereas litter in a comparatively more advanced stage of degradation is characterized by the progressive enhancement of alkyl C signal  
305 suggesting the selective enrichment of long-chain and condensed aliphatic structures, including cutins and suberins from higher plants, or phospholipids from microbial and fungal biomass (Miltner et al., 2012; Panettieri et al., 2013). In this study, the presence of a clear peak of terminal methyl group that accounted for half of the intensity of the methylene group indicated that most of the total alkyl C intensity is due to chains shorter than those expected for cutins and suberins. Alkyl C contribution was higher for smaller fractions, probably explained for this experiment by the microbial growth stimulated by the diffusion  
310 into fine pores of smaller molecules released during the enzymatic breakdown of macromolecules (Ludwig et al., 2015). Similar results were found by Clemente et al. (2011), in which combined analyses of solution state  $^1\text{H}$  NMR and diffusion edited  $^1\text{H}$  NMR unveiled that alkyl contribution to the fine fraction of soils under prairie is mainly ascribed to microbial synthesis rather than preservation of plant material. However, the preservation of plant-derived aliphatic short-chains adsorbed, on mineral surfaces of soil fine particles could not be excluded (Basile-Doelsch et al., 2015).

315 The larger macroaggregates of the three treatments with vegetal inputs were characterized by a high contribution of *O*-alkyl C; in the case of ley grassland, 43% of the total C intensity measured by NMR was assigned to carbohydrates, a value close to that for the non-degraded plant tissue. Fig. 5 shows the alkyl/*O*-alkyl ratios for the four treatments. Trends along the aggregate fractions evidenced how ley grassland had similar ratios than those of permanent grassland for fine fractions, but a totally different ratio for larger macroaggregates, suggesting that this fraction is mainly composed of coarse vegetal material derived  
320 from the recently established maize crop.

### 3.4 Chemical composition of the soil organic matter pools from different land-uses

At this point, the interpretation of the relative abundances of each compound classes obtained from the  $^{13}\text{C}$  NMR spectra and the quantification of LF-C turnover using *in-situ* labelling provided by maize constitutes a valid and original approach to understand how land-use affects the dynamics of SOM pools within different aggregate compartments.

325 A PCA analysis was performed to represent the differences of LF isolated from aggregate fractions of four treatments based  
on the relative abundance of NMR compound classes (Fig. 6). In the plane defined by the two first components (82.5% variance  
explained), the four treatments could be differentiated along the first component, while the second component ordered the  
samples by aggregate size, i.e. coarser fractions on the top of the plot, finer fractions on the bottom. The observations  
corresponding to permanent grassland fractions were clearly placed on the left of the plot, on the opposite side of the bare  
330 fallow ones. Two out of four fraction classes (macroaggregates, silt and clay) may be connected with a quasi-horizontal line  
from left to right following the order permanent grassland–ley grassland–permanent cropland–bare fallow, whereas larger  
macroaggregates and microaggregates had a more scattered distribution. Looking at the position of the different treatments,  
permanent cropland hull was partially overlapped to the hulls described by ley grassland, and with the BS fraction of BF. Ley  
grassland presented the greatest scattering along the second component, meaning that chemical composition of aggregates was  
335 highly different, and it evidenced a prominent shift from the original grassland footprint to the cropland footprint. Similar  
changes occurred in the molecular composition of SOM under ley grassland studied by analytical pyrolysis (Rumpel et al.,  
2009). This result demonstrated that  $^{13}\text{C}$  NMR analyses of LF-C may be useful to detect changes in SOM quality due to land-  
use on a short-term timescale, since this shift of ley grassland samples through a permanent cropland footprint was not detected  
with analyses performed on total SOM from bulk soil on the same experimental area (Crème et al., 2018; Panettieri et al.,  
340 2017).

The active variables of the PCA were split into two groups; on the right part, a cluster formed by the variables aromatic, *O*-  
aryl and carboxyl C was correlated to the first component and had a higher relative contribution to the observations under bare  
fallow, in which no vegetal inputs were returned for nine years. This cluster can be interpreted as an advanced status of  
degradation of the organic matter in the LF associated with the land-use (Leifeld and Kögel-Knabner, 2005). On the left and  
345 more scattered along the second component axis, the variables *O*-alkyl, *N*-alkyl, alkyl and terminal alkyl reflected the different  
composition of SOM based on the different proportion of microbial-derived SOM, maize-derived and grassland-derived inputs.  
The exploration of PCA indicated that the largest distances between homologous fractions of different land-uses were found  
for larger macroaggregates and microaggregates, showing that the four land-uses caused chemical differences of larger  
magnitude within those fractions. The supplementary variables were most effectively described by the  $^{13}\text{C}$  NMR regions *O*-  
350 alkyl, *N*-alkyl and terminal alkyl, plus the cluster of degradation status on the right side of the plot.

The supplementary variables TOC and C/N were placed on the left part of the graph, TOC was correlated to the area described  
by the permanent grassland observation and the *N*-alkyl C, whereas C/N was correlated to the larger macroaggregates and *O*-  
alkyl C. Losses of C3 derived LF-C were placed on the right of the plot, closely correlated to the area of the graph described  
by bare fallow and perfectly opposite (thus negatively correlated) to *N*-alkyl C and terminal alkyl.

355 The fact that losses of LF-C were correlated to the N cycle (in this case, the  $^{13}\text{C}$  NMR signal attributed to proteinaceous  
material) and to the intensity of the terminal methyl group attributed to microbial aliphatic material agrees with recent findings

about the stoichiometric relationships controlling the microbial degradation of vegetal litter (Chen et al., 2019; Sinsabaugh et al., 2013). As a result, the progressive mineralization of fresh litter induces a higher contribution of microbial-derived C to SOM, and a possible redistribution of the C through heavier fractions of SOM. These dynamics appears to be land-use and aggregate-size dependent.

### 3.5 The effect of land-use on the degradation status of organic matter pools

The spectral subtractions with respect to permanent grassland samples were used to define selective losses (positive values) or gains (negative values) in the  $^{13}\text{C}$  NMR intensities for each land-use (Fig. 7).

The results highlighted that LF isolated from bulk soil and most of the aggregate fractions of permanent grassland had a higher contribution of *O*-alkyl C if compared with homologous samples from the other treatments, with the exception of larger macroaggregates in ley grassland and permanent cropland. This trend was compensated with an enrichment in the aromatic, heteroaromatic and carboxylic regions with respect to the intensities registered for permanent grassland soils. When a soil under grassland is left bare for nine years, the quantity of LF-C decreased and  $^{13}\text{C}$  NMR intensity assigned to carbohydrates of LF-C decreased with the size of the aggregates (Panettieri et al., 2014; Plaza et al., 2013; Six et al., 2004). With the exception of larger macroaggregates fractions, the magnitude of these effects increased from ley grassland to permanent cropland to bare fallow, clearly indicating that LF-C of the treatments under maize presented a more degraded status than those under permanent grassland. The LF-C isolated from silt and clay fraction of permanent grassland had also higher intensities in alkyl and terminal alkyl regions. The data also suggest that the LF-C of the silt and clay fraction suffers minor changes related to land-use in terms of quantity, but the  $^{13}\text{C}$  NMR signal intensity attributed to alkyl decreases for this fraction when soil is either cultivated under maize or left bare. The fact that bare fallow presents a similar trend towards lower alkyl contribution than treatments cultivated under maize confirm that this result is mostly attributable to the losses of microbial-derived C presumably rich in short aliphatic chains, rather than to contribution of plant-derived short aliphatic chains, as explained above.

The presence of higher proportion of carbohydrate-derived material in LF-C isolated from large aggregates and the corresponding higher contribution of microbial C in fine fraction agrees with the literature describing the size-dependant reactivity of the aggregates (Puget et al., 1995; Six et al., 2000; Tisdall and Oades, 1982). Large aggregates contain high amounts of fresh plant material rich in carbohydrates that is preferentially degraded by exoenzymes (Baldock and Preston, 1995), the so-called detritusphere. Moreover, aggregates contain the by-products of the enzymatic breakdown of macromolecules, which tends to diffuse into finer pores, sustaining the higher microbial proliferation in finer fractions (Courtier-Murias et al., 2013; Ludwig et al., 2015; Miltner et al., 2012). When not enough macromolecules are degraded in coarser fractions (i.e. lower contribution or lower degradation of polysaccharides), the flux of by-products could be interrupted and this proliferation is not sustained anymore (Plaza et al., 2013). However, when a different vegetal input is returned to the soil after changing land-use (from grassland to permanent maize cropping), losses in alkyl C intensity of LF-C for silt and clay

fraction were also registered for ley grassland and permanent cropland. This could be indicating that the location and the type of inputs had an influence on the alkyl C contribution to this fraction, supporting the idea that alkyl moieties found in this fraction are microbial-derived material (Eclesia et al., 2016). After three years of maize cropping, LF-C from ley grassland showed a higher proportion of carbohydrate derived material (*O*-alkyl) in the larger macroaggregates and a higher contribution of maize-derived LF-C, as assessed by isotopic analyses. Therefore, land-use specific characteristics of the maize phase such as the new type of vegetal input, a different root network or the tillage operation were responsible of a change in quantity and chemical composition of the LF-C from larger macroaggregates under ley grassland (von Haden et al., 2019).

For LF-C extracted from the other fractions of ley grassland, the *O*-alkyl intensities were lower than those of permanent grassland, showing that grassland-derived material is being degraded under maize cropping. A similar trend of *O*-alkyl losses in comparison to permanent grassland was detected for permanent cropland, with the exception of the larger macroaggregates fraction in which the *O*-alkyl intensities were similar in the two treatments. Therefore, we can infer that (i) maize inputs rich in carbohydrates are mostly deposited as surface litter (Panettieri et al., 2017), (ii) maize cropping tended to increase aggregates MWD compared to grassland, and (iii) surface litter lasts in LF-C of larger macroaggregates as non-degraded material three years after land-use change, but a degradation and/or a redistribution to heavier soil fraction is expected on a time scale of nine years.

On the other hand, grassland provides higher belowground inputs resulting in higher amounts of LF-C but in this case lower MWD. The trend to higher aggregates MWD when maize is implemented into the crop rotation may be explained by the differences between the most abundant inputs type under maize and grassland (i.e. coarse maize-derived aboveground inputs and grassland belowground ones). Large contribution of grassland-derived belowground inputs rich in vegetal macromolecules are progressively degraded and redistributed from larger to finer aggregates and that may be feeding and sustaining the microbial growth found in the finest fraction of permanent grassland. As soon as grassland is substituted by maize, the changes in litter traits may hamper this flux of nutrients and the contribution of microbial C to LF-C decreases. Under our experimental conditions, maize derived belowground inputs are less abundant and with different root traits compared to grassland (Panettieri et al., 2017; Armas-Herrera et al., 2016), a larger proportion of coarse aboveground input is returned to the soil and left “untouched” until a new type of detritusphere ecosystem is built around it and the new equilibrium will be reached (Kumar et al., 2016; Kuzyakov and Blagodatskaya, 2015). In fact, the *O*-alkyl C contribution to silt and clay fraction of permanent cropland is higher than that found for ley grassland, demonstrating that the  $^{13}\text{C}$  NMR signal attributed to carbohydrates is restored within a longer timescale.

Comparison of the trends of the three vegetated treatments with those found for bare fallow shows that, despite the new inputs returned to soil under maize, the change in land-use in ley grassland will provoke the disruption of the equilibrium reached under the previous grassland cover. Some of the aggregate fractions of ley grassland will continue to function if the land-use change did not happen, showing a degradation of LF-C in terms of quantity of quality similar to that registered for bare fallow.

420 This may be explained by the fact that land-use specific microenvironments are not adapted to the degradation of the new  
vegetal inputs because of its different chemical characteristics and/or different spatial arrangement (Castellano et al., 2015;  
Eclesia et al., 2016). Later on, the newly built aggregates and microenvironments under the new phase of the rotation will  
become the majority of the total soil matrix, switching the net soil functionality to the new land-use. We suggest that this may  
be one of the explanations for the so-called “legacy effect”, described as the influence of previous land-uses on the soil C  
425 recovery/loss dynamics after the establishment of a new soil management (Compton et al., 1998; Smith, 2014). Moreover, the  
optimum for soil microbial diversity and soil C storage tends to happen at an optimum level of soil perturbation and land-use  
switch following a humped back curve, different for each type of soil (Acosta-Martínez et al., 2008; Tardy et al., 2015). For  
our study, three years of maize cropping in ley grassland affected the LF-C dynamics in a way similar to that observed for bare  
fallow. This is clearly an alert signal that C stocks accumulated under grassland may be hampered by future cropping years  
430 (Sleutel et al., 2006). Nevertheless, C losses were not observed for bulk soil (Crème et al., 2018) and longer times under maize  
tended to restore LF-C pools and increase MWD, but with an overall loss of C stocks (Panettieri et al., 2017). Therefore,  
refining the data on the land-use depending C persistence in soil may be helpful to decide which land-use rotations will be the  
most suitable for C storage strategies (Rumpel et al., 2019).

#### 4 Conclusions

435 This study provides new insights to unveil the land-use dependency of the storage and degradation dynamics that affect reactive  
C pools. Our findings indicate that C under ley grassland is subjected to two different and mostly independent mechanisms:  
the degradation regarding the grassland-derived LF-C and the accumulation of new maize-derived LF-C. Considering the  
difference between grassland species and maize plant, we assume that root architecture of the rhizosphere contributed to the  
change in the chemical nature and spatial distribution of the vegetal inputs returned to soil.  
440 We found evidences that these factors regulated by land-use led to the formation of land-use specific detritospheres in ley  
grassland, each of them with specific LF-C dynamics of redistribution among different pools and mineralization. The microbial  
proliferation suggested by <sup>13</sup>C NMR for LF-C accumulated during the grassland phase is not sustained during the maize phase,  
as if the microenvironments and microbial communities were not sensitive to the new maize inputs returned as coarse material.  
As a whole, results showed that grassland derived LF-C continues to be degraded as if no inputs were returned to soil, whereas  
445 maize-derived material is slowly degraded. We expect that longer maize cropping time will establish a new equilibrium among  
LF-C isolated from aggregates.  
Agricultural intensification in ley grassland provokes firstly a decrease of soil LF-C, then a depletion of total soil C contents.  
The analytical characterization of LF-C is here proposed as a way to evaluate the impact of crop rotations at shorter timescale,

before that soil C contents are hampered. This study enables to generate sufficient evidence and understanding of C dynamics  
450 at fine scale to devise SOC model predictions and policies to sustain C storage under land-use practices.

### Figure captions

**Figure 1.** Lusignan national long-term observatory at the Nouvelle-Aquitaine region France (a); Land-use management of target treatments from 2005-2013 used in this study before the sampling (b). Continuous maize bands were installed in subplots of the T1 and T3 treatments, in addition to bare fallow that have not received fresh organic matter input since the start of the  
455 experimentation in 2005.

**Figure 2.** Light fraction carbon (LF-C) contribution to total organic carbon in bulk soil ( $n=3$ ) and density fractions ( $n=1$ ) for different treatments (PG: permanent grassland, PC: permanent cropping, LG: ley grassland, BF: bare fallow soil). No significant differences between treatments ( $P < 0.05$ ) for bulk samples were found. Error bars show the calculated standard deviations for replicate samples.

460 **Figure 3.** Percentage of maize-derived (C4) light fraction carbon (LF-C) for bulk soils and aggregate fractions under permanent cropland and ley grassland. LMA: larger macroaggregates; MA: macroaggregates; MiA: microaggregates; S+C: silt and clay. \* values of S+C for ley grassland were slightly lower (-0.4%) than those found for permanent grassland, probably due to field variability. Error bars show the calculated standard deviations for replicate samples.

**Figure 4.** C3 and C4 light fraction C contribution to total light fraction C for different treatments and soil fractions. PG: permanent grassland; LG: ley grassland; PC: permanent cropland; BF: bare fallow soil; LMA: larger macroaggregates; MA: macroaggregates; MiA: microaggregates; S+C: silt and clay. No significant differences between treatments ( $P < 0.05$ ) were found for bulk soil samples. Error bars show the calculated standard deviations for replicate samples.

**Figure 5.** The alkyl to *O*-alkyl ratios calculated for light fraction-C isolated from bulk soils and aggregate fractions for the four treatments. LMA: larger macroaggregates; MA: macroaggregates; MiA: microaggregates; S+C: silt and clay.

470 **Figure 6.** Results of principal component analysis applied to  $^{13}\text{C}$  NMR analysis of the C distribution within different aggregate fractions from soils under different land-uses. Projected loadings of the soil measured variables (left) and representation of the light fraction C isolated from aggregate-size fractions of the four different treatments on the plain defined by the two first principal components (right). Labels for samples and variables refer to Tables 1, 2 and 3.



**Figure 7.** Comparisons of  $^{13}\text{C}$  NMR spectra based on subtractions of the spectra obtained from ley grassland (LG), permanent cropland (PC) and bare fallow (BF) samples from the homologous spectra obtained from permanent grassland (PG, first row, used as controls). Spectral regions: carboxyl C (R1), heteroaromatic (R2), aromatic (R3), anomeric (R4), *O*-alkyl (R5), *N*-alkyl (R6), alkyl (R7), terminal alkyl (R8). For graphical reasons, all the intensities of all the resulting spectra were normalized by an arbitrary factor (10000) to fit within the interval of -2 to +40 arbitrary units. The y axis of all the graphs was scaled to the same interval of arbitrary units, except for LMA of ley grassland.

**Figure S1:** Comparison of  $^{13}\text{C}$  NMR spectra from Ramp-CPSP/MAS and Ramp-CP/MAS sequences on soil light fractions. The region assigned to aromatic-C had higher intensity with the Ramp-CPSP/MAS sequence.

### Authors' contribution

Based on the CASRAI's CRediT definitions of contributor roles, the authors contributed to this work as follow.

*Conceptualization:* MP, AC, CR, MFD. *Data curation:* AC, CR, MP, GA. *Formal analysis:* MP, DCM, MFD, CR, GA.

*Funding acquisition:* AC, CR, MP. *Investigation:* MP, DCM. *Methodology:* MP, DCM, CR, MFD. *Project administration:* AC, MP, CR. *Resources:* AC, CR, MFD, GA. *Software:* DCM, GA, MP. *Supervision:* MP, CR, AC. *Validation:* AC, CR, MFD. *Visualization:* MP, GA. *Writing – original draft:* MP. *Writing – review & editing:* DCM, GA, MFD, CR, AC.

### Data availability

The data generated in the framework of the SOERE-ACBB observatory are freely available and accessible after validation of a specific request from the responsible scientist. The data that support the findings of this study are available from the corresponding and lead authors, upon reasonable request.

### Acknowledgments

The authors acknowledge the support of the AgreenSkills fellowship programme which has received funding from the EU's Seventh Framework Programme under grant agreement n° FP7-26719, the AnaEE France - grant agreement n° ANR-11-INBS-0001 and the CNRS-INSU. The lead author Marco Panettieri acknowledges the funding received through the Transnational Access to Research Infrastructures activity in the 7th Framework Programme of the EC under the ExpeER project n° 262060 for conducting the research.

Financial support from the IR-RMN-THC Fr3050 CNRS for conducting the research is gratefully acknowledged. We are deeply indebted to Xavier Charrier for his technical support at the experimental area SOERE-ACBB (Systems of Observation

500 and Experimentation in Environmental Research- Agro-ecosystem, Biogeochemical Cycles and Biodiversity), Valerie Pouteau, Cyril Girardin, and Daniel Billiou for their technical support in the analyses carried out.

## References

- Álvaro-Fuentes, J., López, M. V., Cantero-Martínez, C. and Arrúe, J. L.: Tillage effects on soil organic carbon fractions in Mediterranean dryland agroecosystems, *Soil Sci. Soc. Am. J.*, 72(2), 541–547, doi:10.2136/sssaj2007.0164, 2008.
- 505 Armas-Herrera, C. M., Dignac, M. F., Rumpel, C., Arbelo, C. D. and Chabbi, A.: Management effects on composition and dynamics of cutin and suberin in topsoil under agricultural use, *Eur. J. Soil Sci.*, 67(4), 360–373, doi:10.1111/ejss.12328, 2016.
- Baldock, J. A. and Preston, C. M.: Chemistry of carbon decomposition processes in forests as revealed by solid-state carbon-13 nuclear magnetic resonance, in *Carbon forms and functions in forest soils*, edited by J. M. Kelly and W. W. McFee, pp. 89–117, Soil Science Society of America, Madison, WI., 1995.
- 510 Balesdent, J. and Mariotti, A.: Measurement of soil organic matter turnover using  $^{13}\text{C}$  natural abundance, in *Mass spectrometry of soils*, edited by T. W. Boutton and S. I. Yamasaki, pp. 83–111, Marcel Dekker, New York (USA), 1996.
- Balesdent, J., Mariotti, A. and Guillet, B.: Natural  $^{13}\text{C}$  abundance as a tracer for studies of soil organic matter dynamics, *Soil Biol. Biochem.*, 19(1), 25–30, doi:http://dx.doi.org/10.1016/0038-0717(87)90120-9, 1987.
- Basile-Doelsch, I., Balesdent, J. and Rose, J.: Are Interactions between Organic Compounds and Nanoscale Weathering Minerals the Key Drivers of Carbon Storage in Soils?, *Environ. Sci. Technol.*, 49(7), 3997–3998, doi:10.1021/acs.est.5b00650, 515 2015.
- Bol, R., Poirier, N., Balesdent, J. and Gleixner, G.: Molecular turnover time of soil organic matter in particle-size fractions of an arable soil, *Rapid Commun. Mass Spectrom.*, 23(16), 2551–2558, doi:10.1002/rcm.4124, 2009.
- Bronick, C. J. and Lal, R.: Soil structure and management: A review, *Geoderma*, 124(1–2), 3–22, 2005.
- 520 Castellano, M. J., Mueller, K. E., Olk, D. C., Sawyer, J. E. and Six, J.: Integrating plant litter quality, soil organic matter stabilization, and the carbon saturation concept, *Glob. Chang. Biol.*, 21(9), 3200–3209, doi:10.1111/gcb.12982, 2015.
- Chabbi, A., Kögel-Knabner, I. and Rumpel, C.: Stabilised carbon in subsoil horizons is located in spatially distinct parts of the soil profile, *Soil Biol. Biochem.*, 41(2), 256–261, doi:http://dx.doi.org/10.1016/j.soilbio.2008.10.033, 2009.
- Chen, J., Seven, J., Zilla, T., Dippold, M. A., Blagodatskaya, E. and Kuzyakov, Y.: Microbial C:N:P stoichiometry and turnover depend on nutrients availability in soil: A  $^{14}\text{C}$ ,  $^{15}\text{N}$  and  $^{33}\text{P}$  triple labelling study, *Soil Biol. Biochem.*, 131, 206–216, 525 doi:10.1016/j.soilbio.2019.01.017, 2019.
- Chenu, C., Angers, D. A., Barré, P., Derrien, D., Arrouays, D. and Balesdent, J.: Increasing organic stocks in agricultural soils: Knowledge gaps and potential innovations, *Soil Tillage Res.*, 188, 41–52, doi:10.1016/j.still.2018.04.011, 2019.

- Clemente, J. S., Simpson, A. J. and Simpson, M. J.: Association of specific organic matter compounds in size fractions of soils under different environmental controls, *Org. Geochem.*, 42(10), 1169–1180, doi:10.1016/j.orggeochem.2011.08.010, 2011.
- 530 Compton, J. E., Boone, R. D., Motzkin, G. and Foster, D. R.: Soil carbon and nitrogen in a pine-oak sand plain in central Massachusetts: Role of vegetation and land-use history, *Oecologia*, 116(4), 536–542, doi:10.1007/s004420050619, 1998.
- Courtier-Murias, D., Simpson, A. J., Marzadori, C., Baldoni, G., Ciavatta, C., Fernández, J. M., López-de-Sá, E. G. and Plaza, C.: Unraveling the long-term stabilization mechanisms of organic materials in soils by physical fractionation and NMR spectroscopy, *Agric. Ecosyst. Environ.*, 171, 9–18, doi:10.1016/J.AGEE.2013.03.010, 2013.
- 535 Courtier-Murias, D., Farooq, H., Longstaffe, J. G., Kelleher, B. P., Hart, K. M., Simpson, M. J. and Simpson, A. J.: Cross polarization-single pulse/magic angle spinning (CPSP/MAS): A robust technique for routine soil analysis by solid-state NMR, *Geoderma*, 226–227(1), 405–414, doi:10.1016/j.geoderma.2014.03.006, 2014.
- Crème, A., Rumpel, C., Le Roux, X., Romian, A., Lan, T. and Chabbi, A.: Ley grassland under temperate climate had a legacy effect on soil organic matter quantity, biogeochemical signature and microbial activities, *Soil Biol. Biochem.*, 122, 203–210, doi:10.1016/j.soilbio.2018.04.018, 2018.
- 540 Derenne, S. and Nguyen Tu, T. T.: Characterizing the molecular structure of organic matter from natural environments: An analytical challenge, *Comptes Rendus - Geosci.*, 346(3–4), 53–63, doi:10.1016/j.crte.2014.02.005, 2014.
- Diekow, J., Mielniczuk, J., Knicker, H., Bayer, C., Dick, D. P. and Kögel-Knabner, I.: Carbon and nitrogen stocks in physical fractions of a subtropical Acrisol as influenced by long-term no-till cropping systems and N fertilisation, *Plant Soil*, 268(1), 319–328, 2005.
- 545 Dignac, M.-F., Derrien, D., Barré, P., Barot, S., Cécillon, L., Chenu, C., Chevallier, T., Freschet, G. T., Garnier, P., Guenet, B., Hedde, M., Klumpp, K., Lashermes, G., Maron, P.-A., Nunan, N., Roumet, C. and Basile-Doelsch, I.: Increasing soil carbon storage: mechanisms, effects of agricultural practices and proxies. A review, *Agron. Sustain. Dev.*, 37(2), 14, doi:10.1007/s13593-017-0421-2, 2017.
- 550 Dignac, M. F., Bahri, H., Rumpel, C., Rasse, D. P., Bardoux, G., Balesdent, J., Girardin, C., Chenu, C. and Mariotti, A.: Carbon-13 natural abundance as a tool to study the dynamics of lignin monomers in soil: An appraisal at the Closeaux experimental field (France), *Geoderma*, 128(1–2), 3–17, doi:10.1016/j.geoderma.2004.12.022, 2005.
- Eclesia, R. P., Jobbagy, E. G., Jackson, R. B., Rizzotto, M. and Piñeiro, G.: Stabilization of new carbon inputs rather than old carbon decomposition determines soil organic carbon shifts following woody or herbaceous vegetation transitions, *Plant Soil*, 409(1–2), 99–116, doi:10.1007/s11104-016-2951-9, 2016.
- 555 Elliott, E. T.: Aggregate Structure and Carbon, Nitrogen, and Phosphorus in Native and Cultivated Soils<sup>1</sup>, *Soil Sci. Soc. Am. J.*, 50(3), 627–633, doi:10.2136/sssaj1986.03615995005000030017x, 1986.

- von Haden, A. C., Kucharik, C. J., Jackson, R. D. and Marín-Spiotta, E.: Litter quantity, litter chemistry, and soil texture control changes in soil organic carbon fractions under bioenergy cropping systems of the North Central U.S., *Biogeochemistry*, 143(3), 313–326, doi:10.1007/s10533-019-00564-7, 2019.
- 560 Helfrich, M., Ludwig, B., Buurman, P. and Flessa, H.: Effect of land use on the composition of soil organic matter in density and aggregate fractions as revealed by solid-state  $^{13}\text{C}$  NMR spectroscopy, *Geoderma*, 136(1–2), 331–341, doi:10.1016/j.geoderma.2006.03.048, 2006.
- 565 IPCC: Climate Change 2013: The Physical Science Basis. Contribution of Working Group I to the Fifth Assessment Report of the Intergovernmental Panel on Climate Change, edited by D. Qin, G.-K. Plattner, M. Tignor, S. K. Allen, J. Boschung, A. Nauels, Y. Xia, V. Bex, and P. M. Midgley, Cambridge University Press, Cambridge, United Kingdom and New York, NY, USA., 2013.
- Jackson, R. B., Canadell, J., Ehleringer, J. R., Mooney, H. A., Sala, O. E. and Schulze, E. D.: A global analysis of root distributions for terrestrial biomes, *Oecologia*, 108(3), 389–411, doi:10.1007/bf00333714, 1996.
- 570 Knicker, H.: Solid state CPMAS  $^{13}\text{C}$  and  $^{15}\text{N}$  NMR spectroscopy in organic geochemistry and how spin dynamics can either aggravate or improve spectra interpretation, *Org. Geochem.*, 42(8), 867–890, 2011.
- Knicker, H. and Lüdemann, H. D.: N-15 and C-13 CPMAS and solution NMR studies of N-15 enriched plant material during 600 days of microbial degradation, *Org. Geochem.*, 23(4), 329–341, 1995.
- 575 Knicker, H., Nikolova, R., Dick, D. P. and Dalmolin, R. S. D.: Alteration of quality and stability of organic matter in grassland soils of Southern Brazil highlands after ceasing biannual burning, *Geoderma*, 181–182, 11–21, 2012.
- Kölbl, A. and Kögel-Knabner, I.: Content and composition of free and occluded particulate organic matter in a differently textured arable Cambisol as revealed by solid-state  $^{13}\text{C}$  NMR spectroscopy, *J. Plant Nutr. Soil Sci.*, 167(1), 45–53, 2004.
- Kumar, A., Kuzyakov, Y. and Pausch, J.: Maize rhizosphere priming: field estimates using  $^{13}\text{C}$  natural abundance, *Plant Soil*, 580 409(1–2), 87–97, doi:10.1007/s11104-016-2958-2, 2016.
- Kunrath, T. R., de Berranger, C., Charrier, X., Gastal, F., de Faccio Carvalho, P. C., Lemaire, G., Emile, J. C. and Durand, J. L.: How much do sod-based rotations reduce nitrate leaching in a cereal cropping system?, *Agric. Water Manag.*, 150, 46–56, doi:10.1016/j.agwat.2014.11.015, 2015.
- Kuzyakov, Y. and Blagodatskaya, E.: Microbial hotspots and hot moments in soil: Concept & review, *Soil Biol. Biochem.*, 585 83, 184–199, doi:10.1016/J.SOILBIO.2015.01.025, 2015.
- Lal, R.: Soil carbon sequestration to mitigate climate change, *Geoderma*, 123(1–2), 1–22, doi:10.1016/J.GEODERMA.2004.01.032, 2004.
- Lal, R.: Sequestration of atmospheric CO<sub>2</sub> in global carbon pools, *Energy Environ. Sci.*, 1(1), 86–100, 2008.

- Le Bissonnais, Y.: Aggregate stability and assessment of soil crustability and erodibility: I. Theory and methodology - Stabilité structurale et évaluation de la sensibilité des sols à la battance et à l'érosion: I: Théorie et méthodologie, *Eur. J. Soil Sci.*, 47(4), 425–437, doi:10.1111/j.1365-2389.1996.tb01843.x, 1996.
- Leifeld, J. and Kögel-Knabner, I.: Soil organic matter fractions as early indicators for carbon stock changes under different land-use?, *Geoderma*, 124(1–2), 143–155, doi:http://dx.doi.org/10.1016/j.geoderma.2004.04.009, 2005.
- Lemaire, G., Jeuffroy, M. H. and Gastal, F.: Diagnosis tool for plant and crop N status in vegetative stage. Theory and practices for crop N management, *Eur. J. Agron.*, 28(4), 614–624, doi:10.1016/j.eja.2008.01.005, 2008.
- Lemaire, G., Franzluebbers, A., Carvalho, P. C. de F. and Dedieu, B.: Integrated crop-livestock systems: Strategies to achieve synergy between agricultural production and environmental quality, *Agric. Ecosyst. Environ.*, 190, 4–8, doi:10.1016/j.agee.2013.08.009, 2014.
- Ludemann, H. D. and Nimz, H.: Carbon 13 nuclear magnetic resonance spectra of lignins, *Biochem. Biophys. Res. Commun.*, 52(4), 1162–1169, 1973.
- Ludwig, M., Achtenhagen, J., Miltner, A., Eckhardt, K.-U., Leinweber, P., Emmerling, C. and Thiele-Bruhn, S.: Microbial contribution to SOM quantity and quality in density fractions of temperate arable soils, *Soil Biol. Biochem.*, 81, 311–322, doi:http://dx.doi.org/10.1016/j.soilbio.2014.12.002, 2015.
- Matos, E. S., Freese, D., Mendonça, E. S., Slazak, A. and Hüttl, R. F.: Carbon, nitrogen and organic C fractions in topsoil affected by conversion from silvopastoral to different land use systems, *Agrofor. Syst.*, 81(3), 203–211, doi:10.1007/s10457-010-9314-y, 2011.
- Miltner, A., Bombach, P., Schmidt-Brücken, B. and Kästner, M.: SOM genesis: Microbial biomass as a significant source, *Biogeochemistry*, 111(1–3), 41–55, 2012.
- Minasny, B., Malone, B. P., McBratney, A. B., Angers, D. A., Arrouays, D., Chambers, A., Chaplot, V., Chen, Z.-S., Cheng, K., Das, B. S., Field, D. J., Gimona, A., Hedley, C. B., Hong, S. Y., Mandal, B., Marchant, B. P., Martin, M., McConkey, B. G., Mulder, V. L., O'Rourke, S., Richer-de-Forges, A. C., Odeh, I., Padarian, J., Paustian, K., Pan, G., Poggio, L., Savin, I., Stolbovoy, V., Stockmann, U., Sulaeman, Y., Tsui, C.-C., Vågen, T.-G., van Wesemael, B. and Winowiecki, L.: Soil carbon 4 per mille, *Geoderma*, 292, 59–86, doi:10.1016/J.GEODERMA.2017.01.002, 2017.
- Moni, C., Rumpel, C., Virto, I., Chabbi, A. and Chenu, C.: Relative importance of sorption versus aggregation for organic matter storage in subsoil horizons of two contrasting soils, *Eur. J. Soil Sci.*, 61(6), 958–969, doi:10.1111/j.1365-2389.2010.01307.x, 2010.
- Nannipieri, P. and Eldor, P.: The chemical and functional characterization of soil N and its biotic components, *Soil Biol. Biochem.*, 41(12), 2357–2369, 2009.

- Panettieri, M., Knicker, H., Berns, A. E. E., Murillo, J. M. M. and Madejón, E.: Moldboard plowing effects on soil aggregation and soil organic matter quality assessed by  $^{13}\text{C}$  CPMAS NMR and biochemical analyses, *Agric. Ecosyst. Environ.*, 177, 48–57, doi:10.1016/j.agee.2013.05.025, 2013.
- Panettieri, M., Knicker, H., Murillo, J. M., Madejón, E. and Hatcher, P. G.: Soil organic matter degradation in an agricultural chronosequence under different tillage regimes evaluated by organic matter pools, enzymatic activities and CPMAS  $^{13}\text{C}$  NMR, *Soil Biol. Biochem.*, 78, 170–181, doi:10.1016/j.soilbio.2014.07.021, 2014.
- Panettieri, M., Rumpel, C., Dignac, M.-F. and Chabbi, A.: Does grassland introduction into cropping cycles affect carbon dynamics through changes of allocation of soil organic matter within aggregate fractions?, *Sci. Total Environ.*, 576, doi:10.1016/j.scitotenv.2016.10.073, 2017.
- Plaza, C., Fernández, J. M., Pereira, E. I. P. and Polo, A.: A comprehensive method for fractionating soil organic matter not protected and protected from decomposition by physical and chemical mechanisms, *Clean - Soil, Air, Water*, 40(2), 134–139, 2012.
- Plaza, C., Courtier-Murias, D., Fernández, J. M., Polo, A. and Simpson, A. J.: Physical, chemical, and biochemical mechanisms of soil organic matter stabilization under conservation tillage systems: A central role for microbes and microbial by-products in C sequestration, *Soil Biol. Biochem.*, 57, 124–, 2013.
- Poeplau, C. and Don, A.: Effect of ultrasonic power on soil organic carbon fractions, *J. Plant Nutr. Soil Sci.*, 177(2), 137–140, doi:10.1002/jpln.201300492, 2014.
- Poeplau, C., Don, A., Six, J., Kaiser, M., Benbi, D., Chenu, C., Cotrufo, M. F., Derrien, D., Gioacchini, P., Grand, S., Gregorich, E., Griepentrog, M., Gunina, A., Haddix, M., Kuzyakov, Y., Kühnel, A., Macdonald, L. M., Soong, J., Trigalet, S., Vermeire, M. L., Rovira, P., van Wesemael, B., Wiesmeier, M., Yeasmin, S., Yevdokimov, I. and Nieder, R.: Isolating organic carbon fractions with varying turnover rates in temperate agricultural soils – A comprehensive method comparison, *Soil Biol. Biochem.*, 125, 10–26, doi:10.1016/j.soilbio.2018.06.025, 2018.
- Powlson, D. S., Gregory, P. J., Whalley, W. R., Quinton, J. N., Hopkins, D. W., Whitmore, A. P., Hirsch, P. R. and Goulding, K. W. T.: Soil management in relation to sustainable agriculture and ecosystem services, *Food Policy*, 36, S72–S87, doi:10.1016/J.FOODPOL.2010.11.025, 2011.
- Puget, P., Chenu, C. and Balesdent, J.: Total and young organic matter distributions in aggregates of silty cultivated soils, *Eur. J. Soil Sci.*, 46(3), 449–459, 1995.
- Puget, P., Chenu, C. and Balesdent, J.: Dynamics of soil organic matter associated with particle-size fractions of water-stable aggregates, *Eur. J. Soil Sci.*, 51(4), 595–605, doi:10.1046/j.1365-2389.2000.00353.x, 2000.
- Rabbi, S. M. F., Linser, R., Hook, J. M., Wilson, B. R., Lockwood, P. V., Daniel, H. and Young, I. M.: Characterization of Soil Organic Matter in Aggregates and Size-Density Fractions by Solid State  $^{13}\text{C}$  CPMAS NMR Spectroscopy, *Commun. Soil Sci. Plant Anal.*, 45(11), 1523–1537, doi:10.1080/00103624.2014.904335, 2014.

- Rumpel, C., Chabbi, A., Nunan, N. and Dignac, M. F.: Impact of landuse change on the molecular composition of soil organic matter, *J. Anal. Appl. Pyrolysis*, 85(1–2), 431–434, doi:10.1016/j.jaap.2008.10.011, 2009.
- Rumpel, C., Amiraslani, F., Chenu, C., Garcia Cardenas, M., Kaonga, M., Koutika, L. S., Ladha, J., Madari, B., Shirato, Y., Smith, P., Soudi, B., Soussana, J. F., Whitehead, D. and Wollenberg, E.: The 4p1000 initiative: Opportunities, limitations and  
655 challenges for implementing soil organic carbon sequestration as a sustainable development strategy, *Ambio*, doi:10.1007/s13280-019-01165-2, 2019.
- Scharlemann, J. P., Tanner, E. V., Hiederer, R. and Kapos, V.: Global soil carbon: understanding and managing the largest terrestrial carbon pool, *Carbon Manag.*, 5(1), 81–91, doi:10.4155/cmt.13.77, 2014.
- Shu, J., Li, P., Chen, Q. and Zhang, S.: Quantitative Measurement of Polymer Compositions by NMR Spectroscopy: Targeting  
660 Polymers with Marked Difference in Phase Mobility, *Macromolecules*, 43(21), 8993–8996, doi:10.1021/ma101711f, 2010.
- Sinsabaugh, R. L., Manzoni, S., Moorhead, D. L. and Richter, A.: Carbon use efficiency of microbial communities: stoichiometry, methodology and modelling, edited by J. Elser, *Ecol. Lett.*, 16(7), 930–939, doi:10.1111/ele.12113, 2013.
- Six, J., Paustian, K., Elliott, E. T. and Combrink, C.: Soil structure and organic matter: I. Distribution of aggregate-size classes and aggregate-associated carbon, *Soil Sci. Soc. Am. J.*, 64(2), 681–689, 2000.
- 665 Six, J., Bossuyt, H., Degryze, S. and Deneff, K.: A history of research on the link between (micro)aggregates, soil biota, and soil organic matter dynamics, *Soil Tillage Res.*, 79(1), 7–31, 2004.
- Sleutel, S., De Neve, S., Singier, B. and Hofman, G.: Organic C levels in intensively managed arable soils - long-term regional trends and characterization of fractions, *Soil Use Manag.*, 22(2), 188–196, doi:10.1111/j.1475-2743.2006.00019.x, 2006.
- Smith, P.: Do grasslands act as a perpetual sink for carbon?, *Glob. Chang. Biol.*, doi:10.1111/gcb.12561, 2014.
- 670 Smith, P.: Soil carbon sequestration and biochar as negative emission technologies, *Glob. Chang. Biol.*, 22(3), 1315–1324, doi:10.1111/gcb.13178, 2016.
- Solomon, D., Lehman, J., Kinyangi, J., Amelung, W., Lobe, I., Pell, A., Riha, S., Ngoze, S., Verchot, L., Mbugua, D., Skjemstad, J. and Schafer, T.: Long-term impacts of anthropogenic perturbations on dynamics and speciation of organic carbon in tropical forest and subtropical grassland ecosystems, *Glob. Chang. Biol.*, 13(2), 511–530, doi:10.1111/j.1365-  
675 2486.2006.01304.x, 2007.
- Tisdall, J. M. and Oades, J. M.: Organic matter and water-stable aggregates in soils, *J. Soil Sci.*, 33(2), 141–163, 1982.
- van Bavel, C. H. M.: Mean Weight-Diameter of Soil Aggregates as a Statistical Index of Aggregation1, *Soil Sci. Soc. Am. J.*, 14(C), 20, doi:10.2136/sssaj1950.036159950014000c0005x, 1950.
- Wiesmeier, M., Urbanski, L., Hobbey, E., Lang, B., von Lützow, M., Marin-Spiotta, E., van Wesemael, B., Rabot, E., Ließ, M., Garcia-Franco, N., Wollschläger, U., Vogel, H. J. and Kögel-Knabner, I.: Soil organic carbon storage as a key function of  
680 soils - A review of drivers and indicators at various scales, *Geoderma*, 333, 149–162, doi:10.1016/j.geoderma.2018.07.026, 2019.

Yamashita, T., Flessa, H., John, B., Helfrich, M. and Ludwig, B.: Organic matter in density fractions of water-stable aggregates in silty soils: Effect of land use, *Soil Biol. Biochem.*, 38(11), 3222–3234, doi:10.1016/j.soilbio.2006.04.013, 2006.

## 685 Tables

**Table 1.** Typical assignments for peaks in  $^{13}\text{C}$  NMR solid-state spectra from geochemical samples (Knicker, 2011; Knicker and Lüdemann, 1995). Reference used: Tetramethylsilane = 0 ppm.

<b>Chemical shift range (ppm)</b>	<b>Name of the spectral region</b>	<b>Assignment</b>
210-160	<i>Carboxyl</i>	Carboxyl, carbonyl, ester, and amide carbons.
160 – 140	<i>Heteroaromatic</i>	Aromatic COR or CNR groups, furans.
140 – 110	<i>Aromatic</i>	Aromatic C-H carbons, guaiacyl C-2 and C-6 in lignin, olefinic carbons, bridging C in polyaromatic units.
110 – 90	<i>Anomeric</i>	Anomeric carbon of carbohydrates, syringyl C-2 and C-6 in lignin.
90 – 60	<i>O-alkyl</i>	Carbohydrate-derived structures (C-2 to C-6) in hexoses, C- $\alpha$ of some amino acids, higher alcohols.
60-45	<i>N-alkyl</i>	Methoxyl groups, C- $\alpha$ of most amino acids, N-alkyl C.
45 – 25	<i>Alkyl</i>	Methylene groups in aliphatic rings and chains.
25-0	<i>Terminal alkyl</i>	Terminal methyl groups.



**Table 2.** C-to-N ratios, mean weight diameter (MWD) and  $\delta^{13}\text{C}$  signature measured for the bulk soil and aggregate fractions of four treatments. Significant differences between treatments ( $P < 0.05$ ) for bulk soil samples are indicated with different letters.

<b>Treatment</b>	<b>Fraction</b>	<b>C/N</b>	<b>Mean weight diameter (MWD) mm</b>	<b><math>\delta^{13}\text{C}</math> signature ‰</b>
<i>Permanent cropland</i>	Bulk soil	14.0 ± 2.0		-25.0 ± 0.02 <b>b</b>
	LMA	18.4		-22.9
	MA	15.1	0.70 ± 0.17 <b>b</b>	-24.9
	MiA	13.5		-25.4
	S+C	15.3		-26.3
<i>Ley grassland</i>	Bulk soil	13.9 ± 0.9		-26.6 ± 0.2 <b>ab</b>
	LMA	20.0		-23.6
	MA	18.2	0.66 ± 0.16 <b>ab</b>	-26.1
	MiA	13.1		-25.9
	S+C	14.7		-27.0
<i>Permanent grassland</i>	Bulk soil	13.7 ± 0.7		-27.5 ± 0.2 <b>a</b>
	LMA	14.8		-27.7
	MA	16.4	0.54 ± 0.16 <b>ab</b>	-27.6
	MiA	14.3		-27.4
	S+C	13.7		-26.9
<i>Bare fallow</i>	Bulk soil+	14.7 ± 1.6		-26.9 ± 0.2 <b>ab</b>
	LMA	10.6		-25.5
	MA	12.5	0.40 ± 0.10 <b>a</b>	-26.4
	MiA	15.3		-27.0
	S+C	11.8		-26.6

**Table 3.** Integration values (expressed as a percent of the total spectral area), and signal-area ratios, of the main regions of  $^{13}\text{C}$  NMR spectra from soils under contrasted agricultural management  $\pm$  standard deviations. Significant differences between treatments ( $P < 0.05$ ) for field replicates of bulk soil samples ( $n=3$ ) are indicated with different letters.

		Carboxyl	Hetero-aromatic	Aromatic	Carbohydrates		N-Alkyl or Methoxyl	Alkyl		Carbohydr. TOT	Alkyl TOT	Aryl/O-Aryl
					Anomeric	O-Alkyl		Methylene	Methyl			
Permanent Cropland	Bulk	9.0 $\pm$ 0.9	7.8 $\pm$ 1.0	<b>21.9</b> $\pm$ <b>1.0</b> ab	8.8 $\pm$ 0.1	24.1 $\pm$ 1.3	9.3 $\pm$ 0.5	13.1 $\pm$ 0.8	6.1 $\pm$ 0.6	32.8 $\pm$ 1.2	19.2 $\pm$ 1.3	2.8 $\pm$ 0.2
	LMA	7.0	7.3	20.0	9.8	27.4	9.2	12.7	6.5	37.3	19.2	2.7
	MA	8.3	7.3	21.9	9.0	25.2	9.5	13.0	5.8	34.1	18.8	3.0
	MiA	8.0	7.4	21.6	8.6	24.5	10.1	13.3	6.5	33.1	19.8	2.9
	S+C	8.7	7.24	21.9	8.0	22.5	9.7	14.9	6.9	30.5	21.8	3.0
Ley Grassland	Bulk	8.2 $\pm$ 0.4	7.3 $\pm$ 0.2	<b>21.6</b> $\pm$ <b>0.6</b> ab	8.5 $\pm$ 0.4	24.4 $\pm$ 0.5	9.8 $\pm$ 0.4	13.6 $\pm$ 0.1	6.6 $\pm$ 0.7	33.0 $\pm$ 0.2	20.2 $\pm$ 0.8	3.0 $\pm$ 0.1
	LMA	7.0	5.9	17.8	9.7	33.7	9.3	10.6	6.0	43.4	16.7	3.0
	MA	7.9	7.1	21.6	8.7	26.6	9.6	12.6	5.9	35.3	18.5	3.0
	MiA	8.5	7.6	21.5	9.1	25.0	9.5	12.5	6.3	34.0	18.8	2.8
	S+C	7.9	7.3	21.6	7.8	21.6	9.4	16.3	8.0	29.5	24.4	3.0
Permanent Grassland	Bulk	8.5 $\pm$ 0.4	7.2 $\pm$ 0.4	<b>20.9</b> $\pm$ <b>1.1</b> a	8.4 $\pm$ 0.2	25.6 $\pm$ 2.0	9.7 $\pm$ 0.2	13.1 $\pm$ 0.5	6.5 $\pm$ 0.9	34.1 $\pm$ 1.9	19.6 $\pm$ 1.2	2.9 $\pm$ 0.1
	LMA	6.9	6.3	19.8	9.3	28.5	9.8	12.8	6.6	37.8	19.4	3.1
	MA	7.3	5.7	18.5	8.6	29.6	9.8	12.8	7.6	38.3	20.4	3.2
	MiA	8.0	6.7	19.5	8.4	26.6	10.5	13.1	7.2	34.9	20.3	2.9
	S+C	7.8	6.7	20.2	7.8	22.48	9.8	16.2	9.1	30.2	25.3	3.0
Bare Fallow	Bulk	7.9 $\pm$ 0.7	7.7 $\pm$ 0.3	<b>22.7</b> $\pm$ <b>0.1</b> b	8.7 $\pm$ 0.2	23.4 $\pm$ 0.1	10.0 $\pm$ 0.4	13.4 $\pm$ 0.3	6.1 $\pm$ 0.6	32.1 $\pm$ 0.2	19.5 $\pm$ 0.4	2.9
	LMA	11.3	9.8	24.5	9.4	20.0	8.4	11.2	5.5	29.4	16.6	2.5
	MA	10.3	9.4	23.8	8.9	21.2	8.6	12.3	5.5	30.0	17.8	2.5
	MiA	8.2	8.2	22.8	7.9	22.0	10.3	13.4	7.2	29.9	20.6	2.8
	S+C	9.6	8.5	23.0	8.5	21.0	8.6	13.9	6.8	29.5	20.7	2.7

**Table 4.** Summary of the characteristics of light fraction C isolated from bulk soil and aggregates of ley grassland. A decoupling between SOM dynamics within larger aggregates and fine fractions is highlighted.

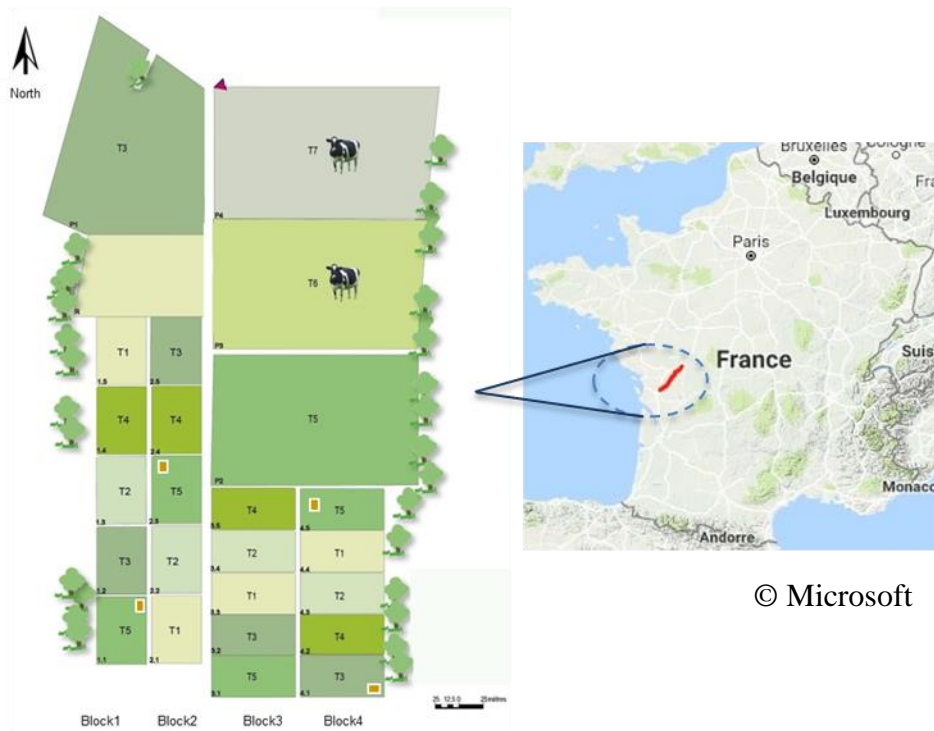
705

<b>Ley grassland fraction</b>	<b><sup>13</sup>C stable isotope probing</b>		<b><sup>13</sup>C NMR</b>	<b>Interpretation</b>
	<i>Maize-derived material</i>	<i>Losses of C3- derived material</i>		
Bulk	Low (5%)	Low	More advanced status of degradation as for BF	LF-C is shifting through a cropland footprint.
LMA	High (30% ≈ PC)	High (PC > PG ≈ BF)	Rich in fresh plant material	New coarse maize input, untouched by C3 feeding microorganisms
MA	Mid (10%)	High (≈ BF)	Low carbohydrates contribution	New maize inputs are low, microorganisms feeds on the scarce C3 remaining
MiA	Mid (10%)	Very high	Low carbohydrates and alkyl chains	Scarce C3 source: microbial growth is not sustained
S+C	None	Low	Microbial proliferation similar to PG	Remaining C3 material sustains a lower microbial proliferation

## Figures

Figure 1.

(a)

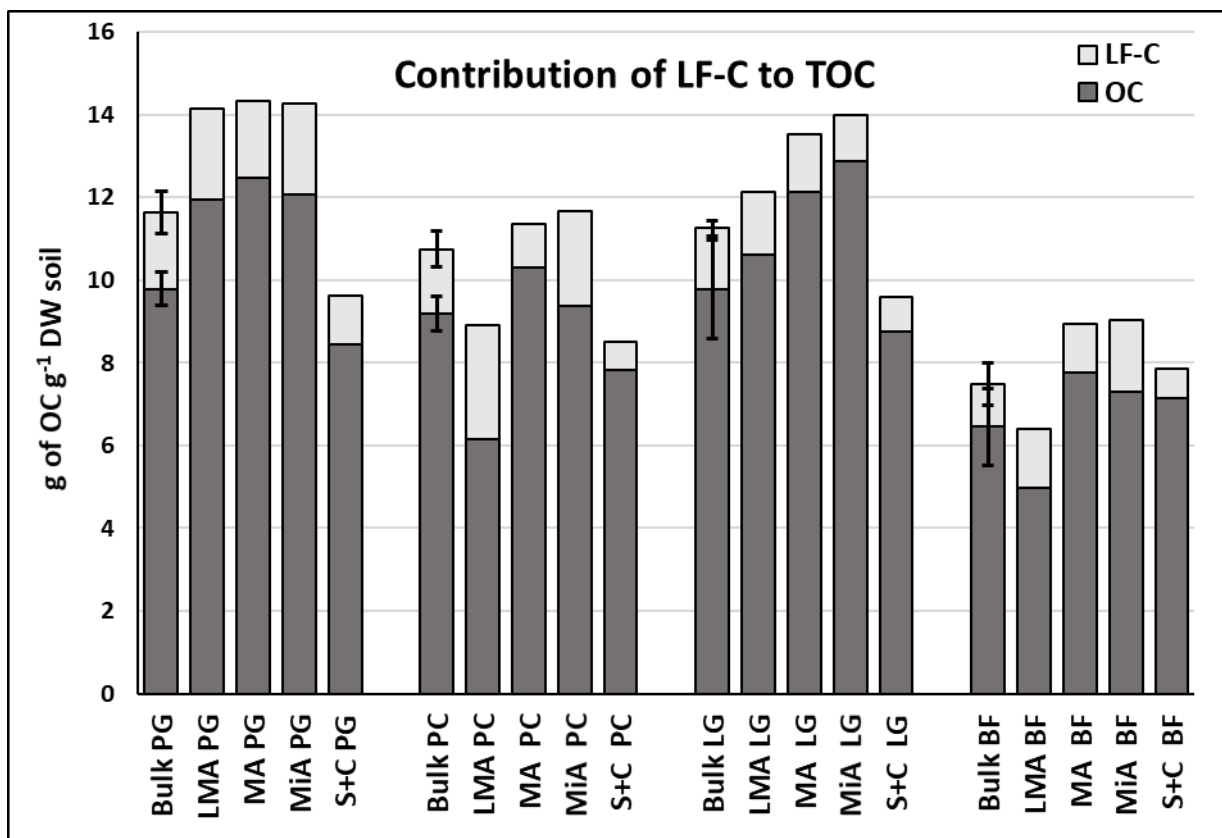


© Microsoft

(b)

		2005	2006	2007	2008	2009	2010	2011	2012	2013
T1	Permanent Cropland	Maize	Maize	Maize	Maize	Maize	Maize	Maize	Maize	Maize
T3	Ley Grassland	Grassland						Maize	Maize	Maize
T5	Permanent Grassland	Grassland								
	Bare Fallow	Bare Fallow								

Figure 2.



715

Figure 3.

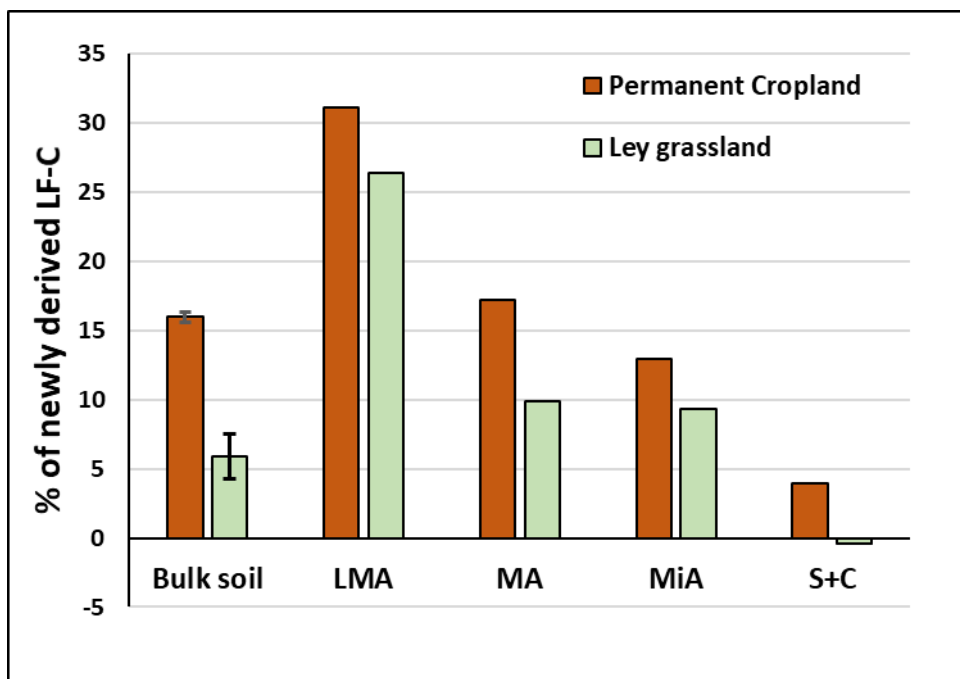
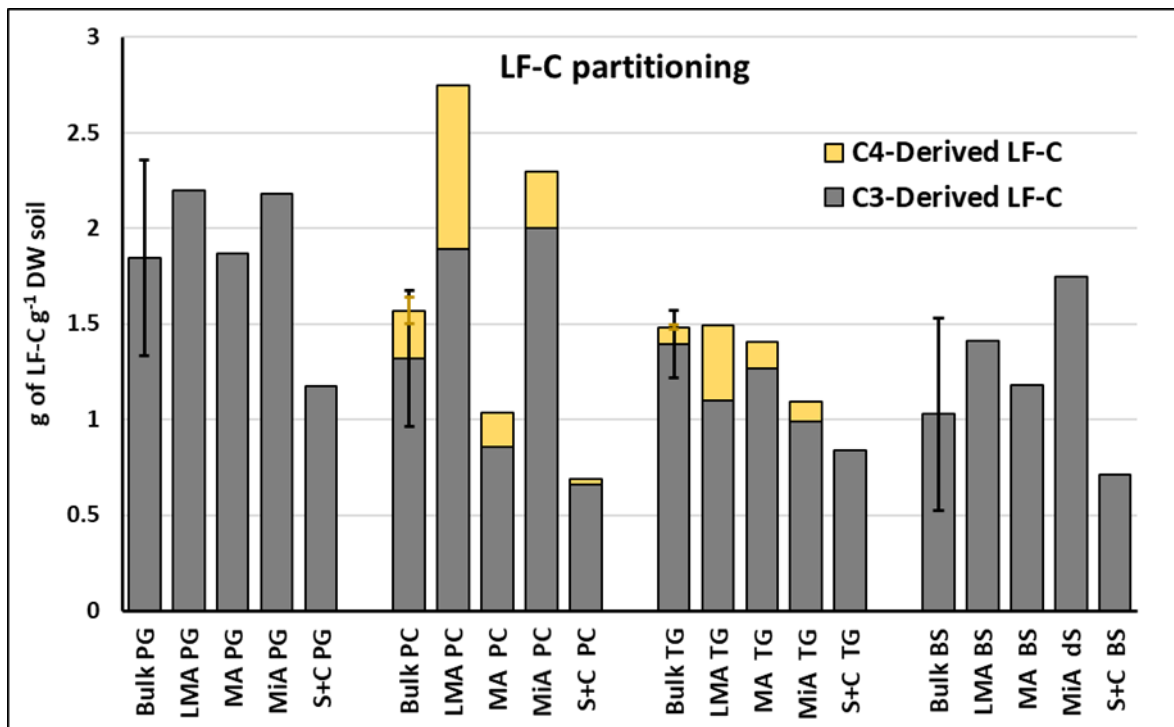


Figure 4.



725 Figure 5.

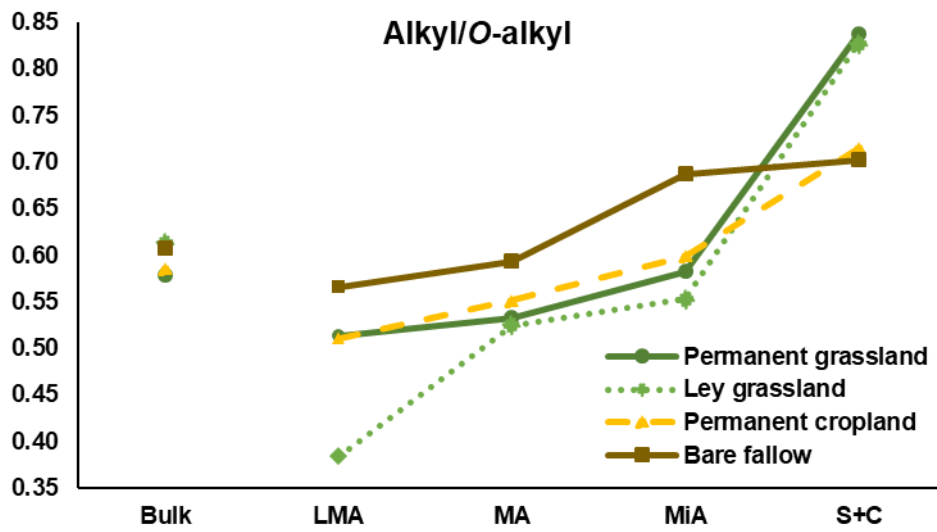




Figure 6.

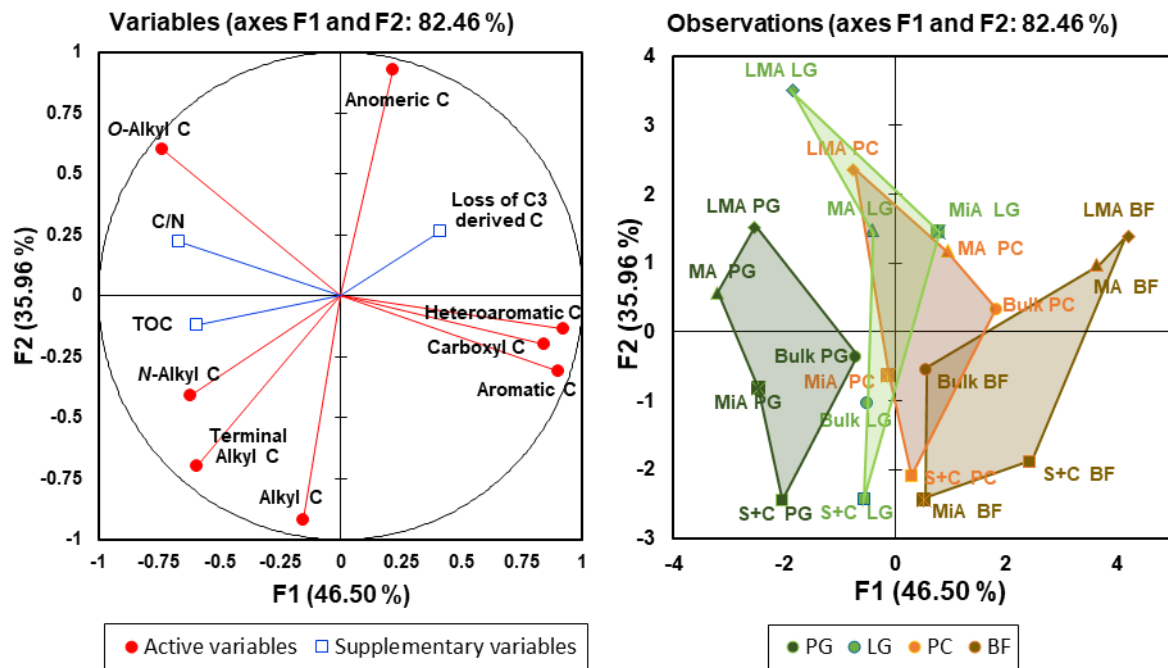


Figure 7.

